



A Novel Sliding Mode Control Method for Tower Crane Systems by Employing Beneficial Disturbance Effects

Menghua Zhang^{1,2}, Xingjian Jing^{2(✉)}, Zaixing Zhu³, Peiran Li⁴, and Lei Chen⁵

¹ School of Electrical Engineering, University of Jinan, Jinan 250000, China

² Department of Mechanical Engineering, The Hong Kong Polytechnic University, Hung Hom, Hong Kong, China

xingjian.jing@polyu.edu.hk

³ Shandong Vocational College of Special Education, Jinan 250000, China

⁴ Shanghai Rockbot Intelligent Technology Pty. Ltd., Shanghai 200333, China

⁵ Power Research Institute of State Grid Ningxia Power Co., Yinchuan 750001, China

Abstract. A novel sliding mode control method, as is shown in this paper, is proposed for the 4-DOF tower crane system by employing beneficial disturbance effects to enhance the transient control performance as well as to ensure the strong robustness simultaneously. More precisely, we deliberately construct a nonlinear disturbance observer, and then, the advantages and disadvantages of the disturbance influence on the 4-DOF tower crane system are described by a constructed disturbance effect indicator (DEI) based on the observation information. Subsequently, the novel sliding mode control method is designed in the light of the estimated disturbance and the introduced DEI. Additionally, the stability of the closed-loop system is demonstrated by Lyapunov techniques. It should be pointed out that the designed method points out that besides bad effects, disturbance has the desirable side-effect of transient control performance improvement, and as a result, introducing desirable side-effect into the controller design is of great importance. The effectiveness and robustness of the designed sliding mode control method can be demonstrated by simulation results.

Keywords: Disturbance effect indicator · Tower cranes · Robustness · Transient control performance · Sliding mode control · Disturbance observer

1 Introduction

In the past few decades, a great deal of efforts have been taken to accurately position the crane and rapidly reduce payload sway. Typical underactuated systems are the crane systems projected to achieve, meaning that the number of independent control inputs is not more than the degrees of freedom (DOFs) [1–5]. The tower crane, enjoying outstanding advantages such as simple structure, convenient installation, low cost, high payload capacity and low energy consumption, is a most extensively used equipment for transporting freights at the construction site [6–8]. Nevertheless, on account of its

unavoidably complicated disturbance, high nonlinearity, and strong underactuation, the design of the tower crane's control system is so far both complicated and challenging. Taking the tower crane's system parameters for example, it is hard to measure them owing to their complicated effect factors. Apart from that, such external disturbances as gust wind also need to be noted owing to its major influence on the stability of the tower crane system. For example, the gust wind may impose an additional payload swing angle. Therefore, we shall take robustness into sufficient consideration in view of its presence of disturbances.

To solve the problems mentioned above, several control methods such as adaptive control [6, 9–11], fuzzy logic control [12, 13] and neural network control [14, 15] have been put forward for the sake of reducing the bounded parametric uncertainties. Furthermore, the powerful robustness as well as the capacity to address unmodeled uncertainties, parametric uncertainties, and external disturbances with driving the sliding surface into 0 is the best known factors of the sliding mode control (SMC) method. As a result, a variety of SMC methods such as integral SMC [16], nonlinear SMC [17, 18], adaptive SMC [17, 19], neural network SMC [20, 21] have been designed for tower crane systems. Recently, several disturbance observer-based control methods have been presented [22–25] to fight off the disturbance effect on the tower crane systems in an even better fashion, which indicate that the disturbance observer-based methods can be used to improve the robustness of the tower crane systems.

However, the tower crane systems' existing control methods are mostly proposed and made an analysis on the basis of the linearized crane model. And this model will differ from the original crane model distinctively if its state variable is not approximate to the equilibrium point. In this sense, it may affect the control performance so much so that the tower crane's stability may be under the influence. Moreover, the positive response aroused by the disturbance are absolutely ignored by the robust control method mentioned above because these methods regard the disturbance as mere detrimental factor, and therefore eliminate it directly. However, we shall note that disturbances may also have certain positive influences [26, 27] given that the fact of mistaking deletion the helpful disturbance may assist us in reflecting the disturbance influence on the tower crane system and thus find an approach to make the most of the helpful disturbance. As a result, given the uncertain or unknown feature of the disturbances, we shall observe them in a nonlinear way in order to evaluate them correctly. After that, a disturbance effect indicator (DEI) shall be specially designed in order to make a distinction between the helping disturbances and the harmful ones based on the estimated disturbances. At the last step, a DEI and the estimated disturbance information will be incorporated into the controller design.

The rest of this paper is indicated as below. In Sect. 2, the problem formulation, including the analysis of the error dynamic mel of 4-DOF tower crane systems as well as the control objective are carried out. In Sect. 3, the main results, embracing design of the nonlinear disturbance observer, introduction of the disturbance effect indicator, and design of the DESMC method, are provided. Several simulation results are illustrated in Sect. 4. The main work of this paper is concluded in Sect. 5.

2 Problem Formulation

2.1 Error Dynamic Model

Control problem of positioning, sway reduction together with inevitable disturbances is taken into account for tower crane systems (shown in Fig. 1), whose dynamical equations are presented as follows:

$$\begin{aligned} & \left[m_p \left(S_1^2 C_2^2 + S_2^2 \right) l^2 + 2m_p x l C_2 S_1 + J + (M_t + m_p) x^2 \right] \ddot{\varphi} - m_p l S_2 \ddot{x} - m_p l^2 C_1 C_2 S_2 \ddot{\theta}_1 \\ & + m_p l (C_2 x + l S_1) \ddot{\theta}_2 + 2(M_t + m_p) x \dot{\varphi} + 2m_p l C_1 C_2 x \dot{\theta}_1 - m_p l S_2 (2\dot{\varphi} S_1 + \dot{\theta}_2) x \dot{\theta}_2 \\ & + 2m_p l S_1 C_2 \dot{\varphi} \dot{x} + m_p l^2 S_{21} C_2^2 \dot{\varphi} \dot{\theta}_1 + m_p l^2 S_1 S_2 C_2 \dot{\theta}_1^2 + m_p l^2 C_1^2 S_{22} \dot{\varphi} \dot{\theta}_2 + 2m_p l^2 C_1 S_2^2 \dot{\theta}_1 \dot{\theta}_2 \\ & = F_\varphi - F_{r\varphi} + d_\varphi \end{aligned} \quad (1)$$

$$\begin{aligned} & - m_p l S_2 \ddot{\varphi} + (M_t + m_p) \ddot{x} + m_p l C_1 C_2 \ddot{\theta}_1 - m_p l S_1 S_2 \ddot{\theta}_2 - (M_t + m_p) x \dot{\varphi}^2 \\ & - 2m_p l C_1 S_2 \dot{\theta}_1 \dot{\theta}_2 - m_p l C_2 \left[S_1 \left(\dot{\varphi}^2 + \dot{\theta}_1^2 + \dot{\theta}_2^2 \right) + 2\dot{\varphi} \dot{\theta}_2 \right] = F_x - F_{rx} + d_x \end{aligned} \quad (2)$$

$$\begin{aligned} & - m_p l^2 C_1 C_2 S_2 \ddot{\varphi} + m_p l C_1 C_2 \ddot{x} + m_p l^2 C_2^2 \ddot{\theta}_1 - m_p l C_1 C_2 (x + l S_1 C_2) \dot{\varphi}^2 \\ & - 2m_p l^2 C_2 (\dot{\varphi} C_1 C_2 + \dot{\theta}_1 S_2) \dot{\theta}_2 + m_p g l S_1 C_2 = 0 \end{aligned} \quad (3)$$

$$\begin{aligned} & m_p l (C_2 x + l S_1) \ddot{\varphi} - m_p l S_1 S_2 \ddot{x} + m_p l^2 \ddot{\theta}_2 + 2m_p l C_2 x \dot{\varphi} + m_p l (x S_1 S_2 - l C_1^2 S_2 C_2) \dot{\varphi}^2 \\ & + 2m_p l^2 C_1 C_2^2 \dot{\varphi} \dot{\theta}_1 + m_p l^2 \dot{\theta}_1^2 S_2 C_2 + m_p g l C_1 S_2 = 0 \end{aligned} \quad (4)$$

where the corresponding system variables, parameters and symbols are illustrated in Table 1.

With a series of experimental measurement, the detailed model of the friction torque and the friction force can be calculated as [1, 19, 22]

$$F_{r\varphi} = F_{r\varphi 1} \tanh(\rho_\varphi \dot{\varphi}) + F_{r\varphi 2} |\dot{\varphi}| \dot{\varphi} \quad (5)$$

$$F_{rx} = F_{rx 1} \tanh(\rho_x \dot{x}) + F_{rx 2} |\dot{x}| \dot{x} \quad (6)$$

where $F_{r\varphi 1}$, $F_{r\varphi 2}$, $F_{rx 1}$, $F_{rx 2}$, ρ_φ and ρ_x standing for friction-related parameters.

For simplicity, Eqs. (1)–(4) are written in the following compact form:

$$\mathbf{M}(\mathbf{q}) \ddot{\mathbf{q}} + \mathbf{C}(\mathbf{q}, \dot{\mathbf{q}}) \dot{\mathbf{q}} + \mathbf{G}(\mathbf{q}) = \mathbf{u} + \mathbf{F}^* \quad (7)$$

wherein $\mathbf{q}[\varphi \ x \ \theta_1 \ \theta_2]^T \in \mathbb{R}^4$ stands for the state vector, $\mathbf{M}(\mathbf{q}) \in \mathbb{R}^{4 \times 4}$ refers to the inertial matrix, $\mathbf{C}(\mathbf{q}, \dot{\mathbf{q}}) \in \mathbb{R}^{4 \times 4}$ represents the Coriolis-centripetal matrix, $\mathbf{G}(\mathbf{q}) \in \mathbb{R}^4$ denotes the gravity vector, $\mathbf{u} \in \mathbb{R}^4$ refers to the control input vector, $\mathbf{F}^* \in \mathbb{R}^4$ represents the disturbance vector. The detailed expressions for $\mathbf{M}(\mathbf{q})$, $\mathbf{C}(\mathbf{q}, \dot{\mathbf{q}})$, $\mathbf{G}(\mathbf{q})$, \mathbf{u} , and \mathbf{F}^* are omitted due to space limitation.

Equations (3) and (4) reflect the coupling relationship between the actuated jib/trolley motion and the unactuated payload swing motion, and the only way to eliminate the

unactuated payload swing angles is to make the best of the coupling relationship. For this purpose, Eq. (7) is divided into the following two parts:

$$\mathbf{M}_{11}\ddot{\mathbf{q}}_1 + \mathbf{M}_{12}\ddot{\mathbf{q}}_2 + \mathbf{C}_{11}\dot{\mathbf{q}}_1 + \mathbf{C}_{12}\dot{\mathbf{q}}_2 = \mathbf{u}_1 + \mathbf{F}_1^* \quad (8)$$

$$\mathbf{M}_{12}\ddot{\mathbf{q}}_1 + \mathbf{M}_{22}\ddot{\mathbf{q}}_2 + \mathbf{C}_{21}\dot{\mathbf{q}}_1 + \mathbf{C}_{22}\dot{\mathbf{q}}_2 + \mathbf{G}_2 = \mathbf{F}_2^* \quad (9)$$

where $\mathbf{q}_1 = [\varphi \ x]^T$ represents the actuated state vector, $\mathbf{q}_2 = [\theta_1 \ \theta_2]^T$ refers to the unactuated state vector. Due to space limitation, the detailed expressions for \mathbf{M}_{11} , \mathbf{M}_{12} , \mathbf{C}_{11} , \mathbf{C}_{12} , \mathbf{F}_1^* , \mathbf{M}_{22} , \mathbf{C}_{21} , \mathbf{C}_{22} , \mathbf{G}_2 , and \mathbf{F}_2^* are omitted.

Table 1. Variables, parameters, and symbols of the 4-DOF tower crane system

Variables/parameters/symbols	Meaning
φ	Slew angle of the jib
x	Displacement of the trolley
θ_1, θ_2	Swing angles of the payload
l	Length of the cable
M_t	Mass of the trolley
m_p	Mass of the payload
J	Inertial moment of the jib
g	Gravitational constant
S_1, S_2, C_1, C_2	Abbreviations of $\sin \theta_1, \sin \theta_2, \cos \theta_1, \cos \theta_2$
d_φ, d_x	Disturbances consist of internal and external disturbances
$F_{r\varphi}$	Friction torque of the jib
F_{rx}	Friction force of the trolley-girder
F_φ	Slew control torque
F_x	Translation control force

It is easy to obtain that $|\mathbf{M}_{22}| > 0$, hence, (9) can be rewritten as follows:

$$\ddot{\mathbf{q}}_2 = -\mathbf{M}_{22}^{-1}\mathbf{M}_{12}\ddot{\mathbf{q}}_1 - \mathbf{M}_{22}^{-1}\mathbf{C}_{21}\dot{\mathbf{q}}_1 - \mathbf{M}_{22}^{-1}\mathbf{C}_{22}\dot{\mathbf{q}}_2 - \mathbf{M}_{22}^{-1}\mathbf{G}_2 + \mathbf{M}_{22}^{-1}\mathbf{F}_2^* \quad (10)$$

It follows from (8) and (10) that

$$\overline{\mathbf{M}}\ddot{\mathbf{q}}_1 + \overline{\mathbf{C}}_1\dot{\mathbf{q}}_1 + \overline{\mathbf{C}}_2\dot{\mathbf{q}}_2 = \mathbf{u}_1 + \mathbf{M}_{12}\mathbf{M}_{22}^{-1}\mathbf{G}_2 + \mathbf{F}_1^* - \mathbf{M}_{12}\mathbf{M}_{22}^{-1}\mathbf{F}_2^* \quad (11)$$

where

$$\begin{aligned} \overline{\mathbf{M}} &= \mathbf{M}_{11} - \mathbf{M}_{12}\mathbf{M}_{22}^{-1}\mathbf{M}_{12} \\ \overline{\mathbf{C}}_1 &= \mathbf{C}_{11} - \mathbf{M}_{12}\mathbf{M}_{22}^{-1}\mathbf{C}_{21} \end{aligned}$$

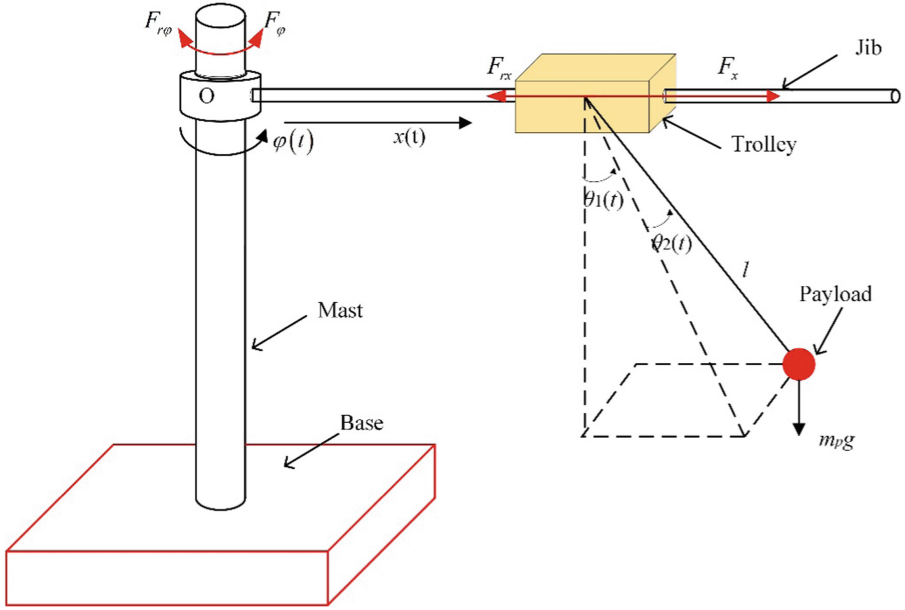


Fig. 1. Schematic diagram of the 4-DOF tower crane system

$$\bar{C}_2 = C_{12} - M_{12} - M_{22}^{-1} C_{22}$$

To further facilitate the following controller design, we define the positioning error vector e as

$$e = [\varphi - \varphi_d \quad x - x_d]^T = [e_\varphi \quad e_x]^T \quad (12)$$

wherein e_φ and e_x refer to the jib and the trolley positioning errors, respectively.

Additionally, we introduce the following sliding surface as

$$s = e + \lambda \dot{e} = [s_1 \quad s_2]^T \quad (13)$$

wherein $\lambda \in \mathbb{R}^{2 \times 2} = \text{diag}(\lambda_1 \quad \lambda_2)$ stands for the positive definite diagonal control matrix.

From Eqs. (11)–(13), it is straightforward to obtain the error dynamic model of the 4-DOF tower crane system as follows:

$$\bar{M}\lambda^{-1}\dot{s} = u_1 + X_1 + X_2 \quad (14)$$

where X_1 stands for the bounded measurable vector, and X_2 refers to the lumped disturbance vector, which are detailed expressed as

$$X_1 = -\bar{C}_1 \dot{q}_1 - \bar{C}_2 \dot{q}_2 + \bar{M}\lambda^{-1} \dot{e} + M_{12} M_{22}^{-1} G_2$$

$$X_2 = F_1^* - M_{12} M_{22}^{-1} F_2^*$$

$$\|\mathbf{X}_2\| \leq N \quad (15)$$

It is easy to conclude that $\|\overline{\mathbf{M}}\| \neq 0$, hence, we can simplify (14) as

$$\dot{\mathbf{s}} = \mathbf{u}_1^* + \mathbf{X}_1^* + \mathbf{X}_2^* \quad (16)$$

where

$$\begin{aligned} \mathbf{u}_1^* &= \lambda \overline{\mathbf{M}}^{-1} \mathbf{u}_1 \\ \mathbf{X}_1^* &= \lambda \overline{\mathbf{M}}^{-1} \mathbf{X}_1 \\ \mathbf{X}_2^* &= \lambda \overline{\mathbf{M}}^{-1} \mathbf{X}_2 \end{aligned}$$

wherein \mathbf{u}_1^* , \mathbf{X}_1^* , and \mathbf{X}_2^* stands for the new control input vector, the new bounded measurable vector, and the new lumped disturbance vector, respectively.

Assumption 1 [1, 6, 8, 11, 19, 22]: Actually, the payload is always kept beneath the jib/trolley, hence, the payload swings are always remained within the following scopes:

$$|\theta_1| < \frac{\pi}{2}, \quad |\theta_2| < \frac{\pi}{2} \quad (17)$$

Assumption 2 [26, 27]: The lumped disturbance vector \mathbf{X}_2^* and its first time derivative $\dot{\mathbf{X}}_2^*$ are both bounded, and \mathbf{X}_2^* , d_φ , d_x converge to 0 as time approach infinity, which can be mathematically expressed as follows:

$$\|\mathbf{X}_2^*\| < \beta, \quad \|\dot{\mathbf{X}}_2^*\| < \alpha, \quad \lim_{t \rightarrow \infty} \mathbf{X}_2^* = 0, \quad \lim_{t \rightarrow \infty} d_\varphi = 0, \quad \lim_{t \rightarrow \infty} d_x = 0 \quad (18)$$

wherein β and α refer to the upper bounds of \mathbf{X}_2^* and $\dot{\mathbf{X}}_2^*$, respectively.

2.2 Control Objective

The final goal is to transport the payload to the desired location quickly and steadily, in the face of uncertain/unknown dynamics and external disturbances. However, as claimed above, arising from the inherent underactuated nature of crane systems, the payload cannot be controlled directly. Therefore, we divide the control objective into two parts:

- 1) Positioning: drive the jib/trolley to the desired angle/position, which can be repressed as

$$\lim_{t \rightarrow \infty} \varphi = \varphi_d, \quad \lim_{t \rightarrow \infty} x = x_d \quad (19)$$

with φ_d as well as x_d standing for the desired jib slew angle and the desired trolley location, respectively.

- 2) Payload swing reduction: reduce the payload swing angles, i.e.

$$\lim_{t \rightarrow \infty} \theta_1 = 0, \quad \lim_{t \rightarrow \infty} \theta_2 = 0 \quad (20)$$

3 Main Results

The overall sliding model control framework is illustrated in this section. Firstly, to estimate the lumped disturbance precisely, a nonlinear disturbance observer is deliberately constructed. Then, a new disturbance effect indicator (DEI) is defined to distinguish beneficial disturbances from bad ones. Finally, a novel sliding mode control method is provided by employing the estimated disturbance information and the introduced DEI.

3.1 Nonlinear Disturbance Observer Design

First and foremost, the observation error vector the lumped disturbance \mathbf{X}_2^* is introduced as follows:

$$\tilde{\mathbf{X}}_2^* = \mathbf{X}_2^* - \hat{\mathbf{X}}_2^* \tag{21}$$

with $\hat{\mathbf{X}}_2^*$ referring to the estimate vector of \mathbf{X}_2^* , $\tilde{\mathbf{X}}_2^*$ standing for the observation error vector.

Subsequently, we construct the following auxiliary function based on the form of (15):

$$\dot{\Gamma}_1 = -L\Gamma_1 + L(-u_1^* - \mathbf{X}_1^* - \Gamma_2) \tag{22}$$

where $L \in \mathbb{R}^{2 \times 2} = \text{diag}(L_1, L_2)$ stands for the positive definite observation gain matrix, and Γ_2 is constructed as follows:

$$\Gamma_2 = Ls \tag{23}$$

The estimate vector $\hat{\mathbf{X}}_2^*$ is then defined as

$$\hat{\mathbf{X}}_2^* = \Gamma_1 + \Gamma_2 \tag{24}$$

Theorem 1: The estimate vector and observation error are all the time maintained within the permissible scopes by using the nonlinear disturbance observer (22)–(24), which can be mathematically described as

$$\|\hat{\mathbf{X}}_2^*\| \leq P_1, \quad \|\tilde{\mathbf{X}}_2^*\| \leq P_2 \tag{25}$$

with P_1 and P_2 referring to upper bounds of the estimate vector $\hat{\mathbf{X}}_2^*$ and the observation error vector $\tilde{\mathbf{X}}_2^*$, respectively. In addition, the observation error vector $\tilde{\mathbf{X}}_2^*$ converges to zero when time approach infinity, in the sense that

$$\lim_{t \rightarrow \infty} \tilde{\mathbf{X}}_2^* = 0 \tag{26}$$

Proof: From (16), (22)–(24), one can obtain that

$$\dot{\hat{\mathbf{X}}}_2^* = \dot{\Gamma}_1 + \dot{\Gamma}_2$$

$$\begin{aligned}
&= -L\Gamma_1 + L(-\mathbf{u}_1^* - \mathbf{X}_2^* - \Gamma_2) + L\dot{s} \\
&= -L\Gamma_1 + L(\mathbf{X}_2^* - \dot{s} - \Gamma_2) + L\dot{s} \\
&= -L\hat{\mathbf{X}}_2^* + L\mathbf{X}_2^*
\end{aligned} \tag{27}$$

It follows from (27) that

$$\begin{aligned}
\hat{\mathbf{X}}_2^* &= \hat{\mathbf{X}}_2^*(0)e^{-Lt} + e^{-Lt} \int_0^t L\mathbf{X}_2^* e^{La} da \\
&\leq \hat{\mathbf{X}}_2^*(0)e^{-Lt} + e^{-Lt} L\beta \int_0^t e^{La} da \\
&\leq \hat{\mathbf{X}}_2^*(0)e^{-Lt} + \beta \\
&\Rightarrow \|\hat{\mathbf{X}}_2^*\| \leq \|\hat{\mathbf{X}}_2^*(0)\| + \beta
\end{aligned} \tag{28}$$

By solving (27), we can also conclude that

$$\begin{aligned}
\tilde{\mathbf{X}}_2^* &= \tilde{\mathbf{X}}_2^*(0)e^{-Lt} + e^{-Lt} \int_0^t \dot{\tilde{\mathbf{X}}}_2^* e^{La} da \\
&\leq \tilde{\mathbf{X}}_2^*(0)e^{-Lt} + e^{-Lt} \alpha \int_0^t e^{La} da \\
&\leq \tilde{\mathbf{X}}_2^*(0)e^{-Lt} + L^{-1}\alpha \\
&\Rightarrow \|\tilde{\mathbf{X}}_2^*\| \leq \|\tilde{\mathbf{X}}_2^*(0)\| + \|L^{-1}\|\alpha
\end{aligned} \tag{29}$$

From (29), as time approach infinity, the observation error vector can be calculated as follows:

$$\lim_{t \rightarrow \infty} \|\tilde{\mathbf{X}}_2^*\| \leq \|L^{-1}\|\alpha \tag{30}$$

$\|L\| \gg \alpha$ is selected in this paper, on which basis, it can be obtained that

$$\lim_{t \rightarrow \infty} \|\tilde{\mathbf{X}}_2^*\| = 0 \rightarrow \lim_{t \rightarrow \infty} \|\hat{\mathbf{X}}_2^*\| = 0 \tag{31}$$

3.2 Disturbance Effect Indicator

As is illustrated in [26], the time-varying disturbances will give rise to the directional property, which has a essentially vital impact on the transient performance of the tower crane system. If the direction of the disturbance is in accordance with the desired motion, the disturbance may have the potential for enhancing the control performance. As a consequence, it is of crucial significance to thoroughly study the relationship between the disturbance influence and the stability/control performance of the controlled system. Here, we give the definition of disturbance effect based on the introduced DEI, which is provided as follows.

Definition 1: For the tower crane error model (16), the DEI is constructed as follows:

$$\chi = \text{sgn}\left(s \circ \hat{\mathbf{X}}_2^*\right) = [\chi_1 \ \chi_2]^T \in \mathbb{R}^2 \quad (32)$$

wherein \circ stands for the element product, based on which, we define the disturbance effect on the error system (16) as

$$\begin{cases} \chi_i > 0 : \text{Disturbance effect is detrimental} \\ \chi_i < 0 : \text{Disturbance effect is beneficial} \\ \chi_i = 0 : \text{Disturbance effect is nill, } i = 1, 2 \end{cases} \quad (33)$$

As we can see from Definition 1, disturbances have negative and positive impacts on the active suspension system. If $\chi_i = 0$, which means disturbances make no difference; if $\chi_i > 0$ and $\chi_i < 0$, disturbances of the system are detrimental and beneficial, respectively. Definition 1 is provided referring to whether the sign of disturbances is in line with the designed motion, and thus it is indispensable to employ the beneficial disturbances to improve the control performance.

3.3 A Novel Sliding Mode Control Method Design and Stability Analysis

First of all, we construct the following non-negative function as follows:

$$V(t) = \frac{1}{2} s^T s \quad (34)$$

Taking the time derivative of (34), and together with the result in (14), one has

$$\begin{aligned} \dot{V}(t) &= s^T \dot{s} \\ &= s^T (\mathbf{u}_1^* + \mathbf{X}_1^* + \mathbf{X}_2^*) \end{aligned} \quad (35)$$

Based on the form of (35), we propose the novel sliding mode control method as follows:

$$\mathbf{u}_1^* = -\mathbf{k}_p s - \mathbf{k}_s \text{sgn}(s) - \|\mathbf{k}_u \mathbf{q}_2\| s - \hat{\mathbf{X}}_2^* \circ \Theta(\chi) \quad (36)$$

with $\mathbf{k}_p = \text{diag}(k_{p1}, k_{p2})$ and \mathbf{k}_s standing for positive control gain matrices, $\text{sgn}(s) = [\text{sgn}(s_1) \ \text{sgn}(s_2)]^T$, $\Theta(\chi) = \text{diag}[\Theta(\chi_1), \Theta(\chi_2)]$, with $\Theta(\chi_i)$, $i = 1, 2$ defined as

$$\Theta(\chi_i) = \begin{cases} 1, & \text{if } \chi_i \geq 0 \\ 0, & \text{if } \chi_i < 0 \end{cases}, \quad i = 1, 2 \quad (37)$$

Additionally, it is easy to conclude from (36) and (37) that

$$\mathbf{u}_1 = \lambda^{-1} \bar{\mathbf{M}} \left[-\mathbf{k}_p s - \mathbf{k}_s \text{sgn}(s) - \|\mathbf{k}_u \mathbf{q}_2\| s - \hat{\mathbf{X}}_2^* \circ \Theta(\chi) \right] \quad (38)$$

Theorem 2: The designed novel sliding mode control method (38) can drive the jib slew angle and the trolley displacement to their desired locations, moreover, simultaneously eliminate the payload swing angles, in the sense that

$$\begin{aligned} \lim_{t \rightarrow \infty} [\varphi \ x \ \theta_1 \ \theta_2]^T &= [\varphi_d \ x_d \ 0 \ 0]^T \\ \lim_{t \rightarrow \infty} [\dot{\varphi} \ \dot{x} \ \dot{\theta}_1 \ \dot{\theta}_2]^T &= [0 \ 0 \ 0 \ 0]^T \end{aligned} \tag{39}$$

Proof: The detailed proof is omitted which is also available upon request.

3.4 Simulation Results and Analysis

In this section, for the purpose of better testing the superior control performance, the designed sliding mode control method, the PD control method [28] and the adaptive control method [6] are chosen as the comparative methods.

After careful tuning, the control gains for all the three control methods are provided in Table 2.

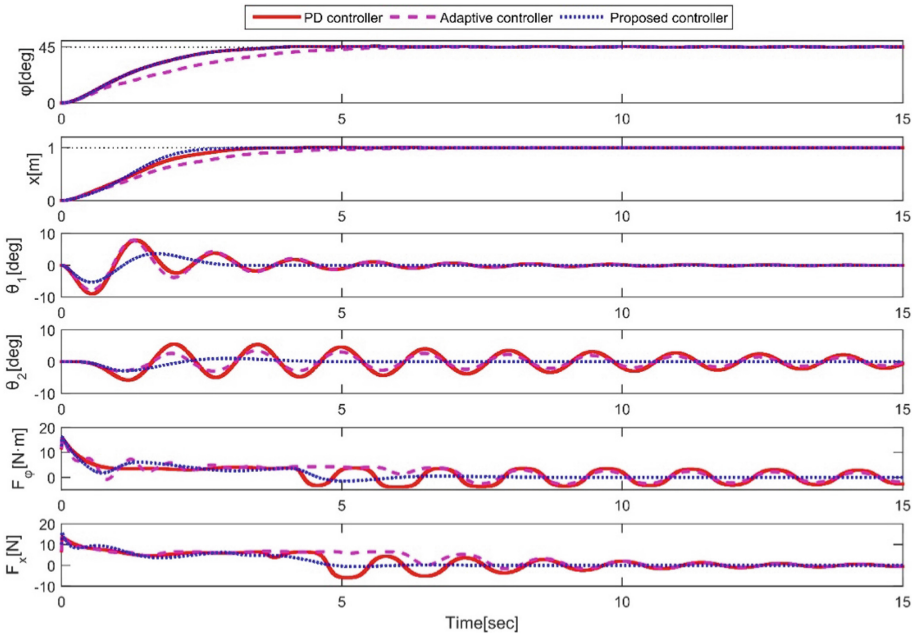


Fig. 2. Simulation results of the designed controller, PD controller, and adaptive controller

The system parameters of the 4-DOF tower crane system are provided as follows:

$$\begin{aligned} M_t &= 3.5 \text{ kg}, m_p = 1 \text{ kg}, l = 0.6 \text{ m}, F_{r\varphi 1} = 4.4, F_{r\varphi 2} = -0.5, \\ \rho_\varphi &= 100, F_{rx1} = 4.4, F_{rx2} = -0.5, \rho_x = 100 \end{aligned}$$

In addition, the initial state vector is set as zero, which can be expressed as

$$\varphi(0) = 0 \text{ deg}, x(0) = 0 \text{ m}, \theta_1(0) = 0 \text{ deg}, \theta_2(0) = 0 \text{ deg}$$

Moreover, the desire jib slew angle and trolley position are set as follows:

$$\varphi_d = 45 \text{ deg}, x_d = 1 \text{ m}$$

Table 2. Control gains

Controllers	Control gains
PD controller	$k_{p\varphi} = 15, k_{d\varphi} = 20, k_{px} = 7, k_{dx} = 10$
Adaptive controller	$k_{p\varphi} = 13.5, k_{d\varphi} = 25, k_{px} = 7, k_{dx} = 12, k_{s\varphi} = 100, k_{sx} = 10$
Proposed controller	$k_{p\varphi} = 16, k_{d\varphi} = 25, k_{px} = 10, k_{dx} = 13.2, k_{s\varphi} = 40,$ $k_{sx} = 10, \mathbf{L} = \text{diag}(100 \ 100), \boldsymbol{\lambda} = \text{diag}(10 \ 15)$

The simulation results of the PD control method, the adaptive control method, and the designed sliding mode control method are plotted in Fig. 2. As far as we can observe from Fig. 2, with similar positioning errors (all within 0.02° and 0.001 m) and transportation time (all within 6 s), the payload swing angles of the designed sliding mode control method can be better suppressed compared with those of the PD control method and the adaptive control method. Furthermore, we can also notice that the payload still swings back and forth after the jib and the trolley stop for the PD control method as well as the adaptive control method, while the payload is almost static for the designed sliding mode control method. In addition, the energy consumption of the designed DESMC method is further less than that of the comparative control methods. Therefore, we can arrive at a conclusion that the designed sliding mode control method can achieve superior control performance, which is also directly obtained from these simulation results.

4 Conclusion

In this paper, in the presence of model uncertainties and external disturbances, a novel sliding mode control method is designed for the 4-DOF tower crane system. First of all, a nonlinear disturbance observer is constructed to precisely observe the lumped disturbance, and subsequently the sliding mode control method is proposed derived from the defined DEI and the estimated disturbance information. It should be pointed out that, in contrast to completely considering the disturbance as bad element of existing control methods for tower crane systems, the designed sliding mode control method takes best advantages of the beneficial disturbance effect, triggering superior control performance. As a consequence, the proposed sliding mode control method can address the inevitable disturbance in a more wise way. The benefit of the proposed sliding mode control method is tested by simulation results.

Acknowledgements. This work was supported in part by the Key Research and Development (Special Public-Funded Projects) of Shandong Province (2019GGX104058), the National Natural Science Foundation for Young Scientists of China (61903155), the General Research Fund of HK RGC (15206717), the funding for Projects of Strategic Importance of The Hong Kong Polytechnic University (1-ZE1N), the Project of Innovation and Technology Fund (K-ZPCN), Natural Science Foundation for Young Scientists of Shandong Province (ZR2019QEE019) and the Doctoral Scientific Fund Project (xbs1910).

References

1. Zhang M, Zhang Y, Chen H, Cheng X (2019) Model-independent PD-SMC method with payload swing suppression for 3D overhead crane systems. *Mech Syst Signal Process* 129:381–393
2. Sun N, Yang T, Fang Y, Wu Y, Chen H (2018) Transportation control of double-pendulum cranes with a nonlinear quasi-PID scheme: design and experiments. *IEEE Trans Syst Man Cybern Syst.* <https://doi.org/10.1109/TSMC.2018.2871627>
3. Zhang M, Jing X, Wang G (2020) Bioinspired nonlinear dynamics-based adaptive neural network control for vehicle suspension systems with uncertain/unknown dynamics and input delay. *IEEE Trans Ind Electron* (in press). <https://doi.org/10.1109/TIE.2020.3040667>
4. Zhang M, Jing X (2021) A bioinspired dynamics-based adaptive fuzzy SMC method for half-car active suspension systems with input dead zones and saturations. *IEEE Trans Cybern.* <https://doi.org/10.1109/TCYB.2020.2972322>
5. Iles S, Matusko J, Kolonic F (2018) Sequence distributed predictive control of a 3D tower crane. *Control Eng Pract* 79:22–35
6. Sun N, Fang Y, Chen H, Lu B, Fu Y (2016) Slew/transportation positioning and swing suppression for 4-DOF tower cranes with parametric uncertainties: design and hardware experimentation. *IEEE Trans Industr Electron* 63(10):6407–6418
7. Bock M, Kugi A (2014) Real-time nonlinear model predictive path-following control of a laboratory tower crane. *IEEE Trans Control Syst Technol* 22(4):1461–1473
8. Kolathaya S (2020) Local stability of PD controlled bipedal walking robots. *Automatica* 114:108841
9. Park MS, Chwa D, Eom M (2014) Adaptive sliding-mode antisway control of uncertain overhead cranes with high-speed hoisting motion. *IEEE Trans Fuzzy Syst* 22(5):1262–1271
10. Wu Y, Sun N, Chen H, Fang Y (2020) Adaptive output feedback control for 5-DOF varying-cable-length tower cranes with cargo mass estimation. *IEEE Trans Ind Inform.* <https://doi.org/10.1109/TII.2020.3006179>
11. Chen H, Fang Y, Sun N (2019) An adaptive tracking control method with swing suppression for 4-DOF tower crane systems. *Mech Syst Signal Process* 123:426–442
12. Wu TS, Karkoub M, Wang H, Chen HS, Chen TH (2016) Robust tracking control of MIMO underactuated nonlinear systems with dead-zone band and delayed uncertainty using an adaptive fuzzy control. *IEEE Trans Fuzzy Syst* 25(4):905–918
13. Wang D, He H, Liu D (2018) Intelligent optimal control with critic learning for a nonlinear overhead crane system. *IEEE Trans Industr Inf* 14(7):2932–2940
14. Yang T, Sun N, Chen H, Fang Y (2020) Neural network-based adaptive antiswing control of an underactuated ship-mounted crane with roll motions and input dead zones. *IEEE Trans Neural Netw Learn Syst* 31(3):901–914
15. Jin Y, Shan C, Wu Y, Xia Y, Zhang Y, Zeng L (2019) Fault diagnosis of hydraulic seal wear and internal leakage using wavelets and wavelet neural network. *IEEE Trans Instrum Meas* 68(4):1026–1034

16. Aboserre LA, El-Badawy AA (2021) Robust integral sliding mode control of tower cranes. *J Vib Control* (in press). <https://doi.org/10.1177/1077546320938183>
17. Kim GH, Hong KS (2019) Adaptive sliding-mode control of an offshore container crane with unknown disturbances. *IEEE/ASME Trans Mechatron* 24(6):2850–2861
18. Liu Z, Sun N, Wu Y, Xin X, Fang Y (2021) Nonlinear sliding mode tracking control of underactuated tower cranes. *Int J Control Autom Syst* 19:1065–1077. <https://doi.org/10.1007/s12555-020-0033-5>
19. Zhang M et al (2018) Adaptive proportional-derivative sliding mode control law with improved transient performance for underactuated overhead crane systems. *IEEE/CAA J Automatica Sinica* 5(3):683–690
20. Tuan LA, Cuong HM, Trieu PV, Nho LC, Thuan VD, Anh LV (2018) Adaptive neural network sliding mode control of shipboard container cranes considering actuator backlash. *Mech Syst Signal Process* 112:233–250
21. Le VA, Le HX, Nguyen L, Phan MX (2019) An efficient adaptive hierarchical sliding mode control strategy using neural networks for 3D overhead cranes. *Int J Autom Comput* 16(5):614–627
22. Qian Y, Fang Y (2018) Switching logic-based nonlinear feedback control of offshore ship-mounted tower cranes: a disturbance observer-based approach. *IEEE Trans Autom Sci Eng*. <https://doi.org/10.1109/TASE.2018.2872621>
23. Wu X, Xu K, Lei M, He X (2020) Disturbance-compensation-based continuous sliding mode control for overhead cranes with disturbances. *IEEE Trans Autom Sci Eng* 17(4):2182–2189
24. Chen W, Saif M (2008) Output feedback controller design for a class of MIMO nonlinear systems using high-order sliding-mode differentiators with application to a laboratory 3D crane. *IEEE Trans Ind Electron* 55(11):3985–3996
25. Kaneko T, Mine H, Ohishi K (2009) Anti sway crane control based on sway angle observer with sensor-delay correction. *IEEJ Trans Ind Appl* 129(6):555–563
26. Guo Z, Guo J, Zhou J, Chang J (2019) Robust tracking for hypersonic reentry vehicles via disturbance estimation-triggered control. *IEEE Trans Aerosp Electron Syst*. <https://doi.org/10.1109/TAES.2019.2928605>
27. Guo Z, Guo J, Zhou J, Zhao J, Zhao B (2018) Reentry attitude tracking via coupling effect-triggered control subjected to bounded uncertainties. *Int J Syst Sci* 49(12):2571–2585
28. Khalil HK (2002) *Nonlinear systems*, 3rd edn. Prentice-Hall, Englewood Cliffs